ISSN 0554-6397
UDK: 004.032.26
Original scientific paper
Received: 30.10.2019.

Sandi Baressi Šegota
E-mail: sbaressisegota@riteh.hr
Nikola Anđelić
E-mail: nandelic@riteh.hr
Faculty of Engineering Rijeka, University of Rijeka, 51000 Rijeka, Croatia
Jan Kudláček
E-mail: jan.kudlacek@fs.cvut.cz
Czech Technical University of Prague, Zikova 1903/4, 166 36 Prague 6, Czech Republic
Robert Čep
E-mail: rober.cep@vsb.cz
VŠB – Technical University of Ostrava, 17. listopadu 2172/15, 708 00 Ostrava, Czech Republic

Artificial neural network for predicting values of residuary resistance per unit weight of displacement

Abstract

This paper proposes the usage of an Artificial neural network (ANN) to predict the values of the residuary resistance per unit weight of displacement from the variables describing ship's dimensions. For this purpose, a Multilayer perceptron (MLP) regressor ANN is used, with the grid search technique being applied to determine the appropriate properties of the model. After the model training, its quality is determined using R^2 value and a Bland-Altman (BA) graph which shows a majority of values predicted falling within the 95% confidence interval. The best model has four hidden layers with ten, twenty, twenty and ten nodes respectively, uses a relu activation function with a constant learning rate of 0.01 and the regularization parameter L2 value of 0.001. The achieved model shows a high regression quality, lacking precision in the higher value range due to the lack of data.

Keywords: artificial intelligence, machine learning, residuary resistance, artificial neural network, multilayer perceptron

1. Introduction

Residuary resistance is the sum of the wave-making resistance and eddy resistance that opposes the movement of a vessel through the water [1]. It can also be defined as the total fluid resistance (drag) without the frictional resistance included [2]. Measurement of the residuary resistance per unit weight of displacement is complex. The used data

set proposes the determination of that value from measurements of ship's dimensions, which are easier to determine and can be achieved using regression methods [3, 4]. While there are many regression methods, this paper proposes the use of an ANN, more precisely an MLP regressor to model the regression. ANNs are a machine learning algorithm [5-7] and such and similar algorithms, like genetic algorithms [8, 9], have been used to a great effect in maritime applications [10, 11]. The wide usage of ANNs can be observed in many research fields, including various marine systems. ANNs can be used in the analysis of marine propulsion systems of any kind [12-16]. Leakage through labyrinth seals can be investigated and optimized using ANNs for both marine [17] and land-based steam turbines [18]. Operation dynamics and losses during the operation can also be tracked by applying ANNs for various components and elements [19-22]. Therefore, the usage of ANNs is not limited to only one (or a few) engineering fields; they can be used in any engineering aspect or problem. The trained ANN model should be capable of determining the value of the residuary resistance per unit weight of displacement from six input variables. As the determination of the parameters the ANN will use is a complex task, a grid search method will be used to help determine them.

1.1. State of the art

Lazarevska (2018) [23] shows the use of various techniques, including fuzzy logic methods. The author concludes that all methods show satisfying results, with the ANN based on the extreme learning machine showing best results. Forrisdal (2018) [24] shows the use of ANNs in predicting the residuary resistance in fast catamarans. Obreja and Chirosca (2018) [25] show the classical determination of the hydrodynamic resistance, and conclude that the level of accuracy isn't satisfactory. Lee et al. (2018) [26] propose the use of genetic programming for the determination of the added resistance in ship hulls, by determining a nonlinear mathematical function describing it. The authors then compare the results with the experimental data. The authors conclude that genetic programming can be used for the prediction of the added hydrodynamic resistance. Yan and Chen (2019) [27] show the use of the Lattice Botzmann method for the calculation of hydrodynamics coefficients. The numerical simulation work load is significantly reduced by the proposed method.

This paper is trying to determine whether the grid search method can be applied to determine the parameters of the MLP for regressive prediction of the residuary resistance and whether such ANN can be used to successfully predict the value of the residuary resistance from the values of variables given in the data set.

2. Methodology and resources

2.1. Data Set

The data set containing training and testing data is obtained from the UCI machine learning depository [28]. The data set consists of 308 data points, each consisting of seven parameters. The data were obtained from full-scale experiments performed at the Delft Ship Hydromechanics Laboratory, and include 22 different hull forms, derived from a parent closely related to the Standfast 43^{TM} designed by Frans Maas [2, 29]. Out of the seven parameters six are inputs and one is output. The inputs include:

- Longitudinal position of the center of buoyancy,
- prismatic coefficient,
- length-displacement ratio,
- beam-draught ratio,
- length-beam ratio and
- Froude number.

While the measured variable, the value of which we are trying to predict, is the residuary resistance per unit weight of displacements, all the variables are non-dimensional. Longitudinal position of the center of buoyancy is the position of the center of mass of the immersed ship measured along its length [19], the prismatic coefficient is the ratio of the volume of displacement of a ship to that of a prism equal in length to the distance between perpendiculars of the ship and in cross section to that of the immersed mid-ship section [30, 31], the length-displacement ratio is the ratio between the length and the displacement of the vessel [32], the beam-draught ratio is the ratio between the lengths of the widest point at the ship's nominal waterline and the draft of the ship [32, 33], the length-beam ratio is the ratio between the length of the vessel and its beam [34], and the Froude number is the ratio of the flow inertia to the external field [35, 36]. The residuary resistance per unit weight of displacement allows shipbuilders to determine the required propulsive power [37-39]. The distribution of values of the output variable in the data set is given in the histogram shown in Figure 1.

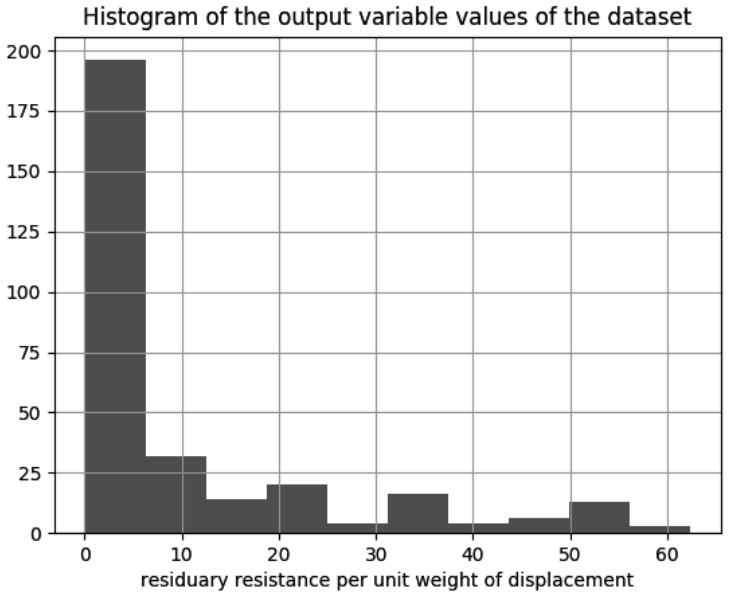

Figure 1 - Histogram showing the distribution of values of the output variable contained within the data set

2.2. MLP Regression

To predict the value of the residuary resistance per unit weight of displacement a MLP ANN is used for regression. MLP is a fully connected feedforward ANN consisting of an input layer, output layer, and one or more hidden layers [40, 41]. When used for regression, the output layer consists of a single node that will provide, after the training is performed and data are placed in the input layer, the value of the variable being predicted [42]. The input layer has the same amount of nodes as the number of input variables - that means six input nodes in the observed case [43]. The number of hidden layers and nodes in each of them is determined along with other parameters, using the grid search method [44].

The grid search method is a method of finding the adequate parameters of the ANN. First, the parameters that will have values adjusted are selected [45]. In this paper the parameters selected were the number of hidden layers along with the number of nodes in each hidden layer [46], the activation function that is a function that defines a node's output based on its input [47, 48], the learning rate type between the constant one (the value remains the same as the initial one), the adaptive one (value changes over time) and the invscaling one (value changes as with the adaptive one, but drops

where it would grow with the adaptive setting) [46, 49], the initial value of the learning rate [50], and the regularization parameter L2 [51]. The learning rate defines how fast the ANN learns. When selecting this value the loss of the ANN has to be taken in consideration. The loss of ANN can be defined as [46]

$$L(X;W,b), \tag{1}$$

then the next iteration weight of the connections of the ANN can be calculated as

$$W_{i+1} = W_i - \eta \Delta L, \tag{2}$$

where η represents the learning rate [52]. If the learning rate is too high, the ANN will reach the regularization goal quickly, but it will have high variance, making new data fit poorly. If the learning rate is too low the goal won't be reached [53]. The L2 regularization parameter adds an L2 penalty equal to the square of the magnitude of coefficient [46, 53]. This regularization serves to avoid over fitting by penalizing high-valued input variables, reducing their value and simplifying the model [46]. Possible parameter values are provided in Table 1. In addition to mentioned parameters two more parameters of the ANN are set – the maximum iteration that defines the maximal number of training iterations of the ANN, and the solver that defines the solver used by the ANN to calculate any necessary values during the training. These parameters are constant throughout the training and are set to 10000 for the number of maximum iterations and the solver used is an Adam solver based on the stochastic gradient descent, with adaptive moment estimation [54].

Table 1 - Parameter values used in grid search for training the ANN

Parameter	Possible values
Hidden layer list	(4,4,4,4),(4,4),(5,4,4,5),(5,4,5),(10,10,10,10,10), (5), (7,7,7,7), (7,7), (10,20,20,10),(6), (12,12,12), (100)
Activation function	'relu', 'identity', 'logistic', 'tanh'
Learning rate type	'constant', 'adaptive', 'invscaling'
Initial learning rate	0.1,0.01,0.5, 0.00001
L2 regularization parameter	0.01,0.1,0.001, 0.0001

In the grid search all possible combinations are searched. From the above table, the number of possible combinations of the parameters can be calculated - there are 2304 possible parameter combinations. For each combination of the above parameters the model is trained. A new model is trained with the same set of parameters a total of 10 times. Training is performed on 75% of the data from the data set (total of

231 measurements), the so called training subset. Once the training of the model is finished, the model is evaluated using the remaining 25% of the data set (total of 77 measurements), which is called a testing subset and the model quality is determined [55]. If the initial model quality is satisfactory, the model is saved for further testing. To determine the model quality coefficient o determination (R^2) is used. R^2 is defined as the proportion of the variance in the dependent variable predictable from the independent variables. It gives information about the goodness of the fit of the model - how well the regression predictions approximate the real data points [56, 57]. R^2 is the element of [0,1], with 1.0 being the best possible score [57]. In this paper only models with an R^2 value greater than 0.97 are stored for further evaluation.

2.3. Bland-Altman analysis

To further determine the quality of the results a Bland-Altman (BA) analysis is performed. The BA analysis is used to compare the results provided by two methods measuring the same parameter, or comparing the predicted versus real data in such instances as the ANN regression. The BA plot is constructed by taking two sets of data X and Y, provided by two methods [58] - in our case the results of real life experiments stored in the data set and the regression ANN predictions. Then, for each data point in these two sets their mean is calculated as [59]

$$p_i = \frac{X_i + Y_i}{2} \tag{3}$$

and the difference between each data point is calculated per

$$d_i = X_i - Y_i. \tag{4}$$

The data points of for each measurement i are then plotted as a scatter plot. On the same plot the bias d, or the mean difference of each measurement is plotted using

$$d = \frac{1}{N}\sum_{i=1}^{N} d_i. \tag{5}$$

The lower and upper bounds of the confidence interval are determined as

$$LOA_l = d - 1.96 s_d \tag{6}$$

and

$$LOA_u = d + 1.96 s_d, \tag{7}$$

where s_d is the standard deviation of the d_i data set. In equations (6) and (7) 1.96

corresponds to the confidence interval of 95%. The BA informs how well the data obtained from the neural network compare to the real data - giving the number of predictions that do not fall within the confidence interval when compared to the real data. The BA also provides information on where those data are located, in terms of values of data points, giving information in terms of precision dependent on the value of the measurement [60].

3. Research results

Out of 20340 models used, 116 models satisfy the condition of $R^2>0.97$. The number of each of the variations of parameters present in those models is shown in Table 2, as well as presented in Figure 2-5. All 116 models that have satisfied the condition had the initial learning rate of 0.01.Parameter variations that weren't present in the models that satisfied the condition aren't shown.

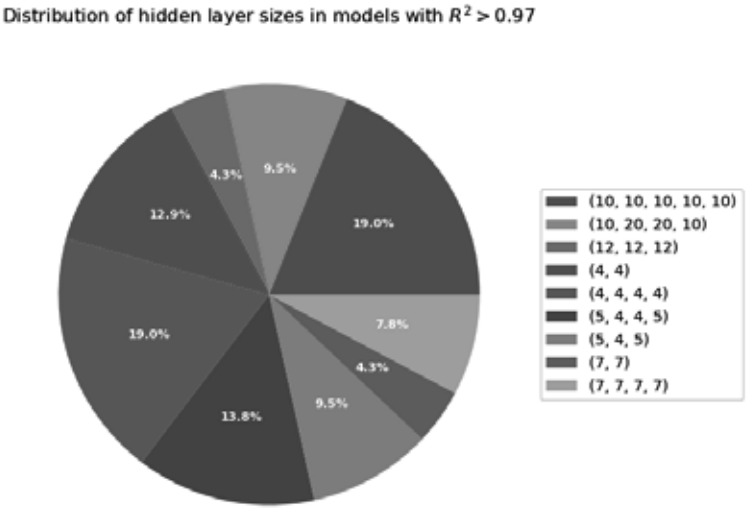

Figure 2 - Distribution of hidden layer sizes variations in the 116 models that satisfy the condition

Table 2 – The number of variations for each of the parameters in models with R2>0.97. The first column shows the parameter that varies while performing the grid search, and the following columns show the parameter value and the number of models out of the 116 satisfying the set condition that use the parameter value in the row above it

Hidden Layer Sizes	(10,10, 10,10,10)	(10,20, 20,20)	(12,12,12)	(4,4)	(4,4,4,4)	(5,4,4,5)	(5,4,5)	(7,7)	(7,7,7,7)	Parameter value
	22	11	5	15	22	16	11	5	9	Number of models
Activation Function	logistic			relu			tanh			Parameter value
	2			97			17			Number of models
Learning rate type	adaptive			constant			invscaling			Parameter value
	45			46			25			Number of models
Initial learning rate	0.01									Parameter value
	116									Number of models
L2	0.0001		0.001		0.01		0.1			Parameter value
	17		30		32		37			Number of models

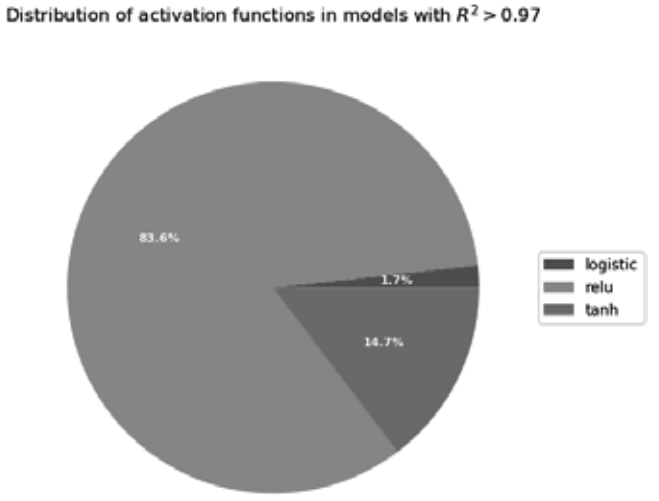

Figure 3 - Distribution of activation function variations in the 116 models that satisfy the condition

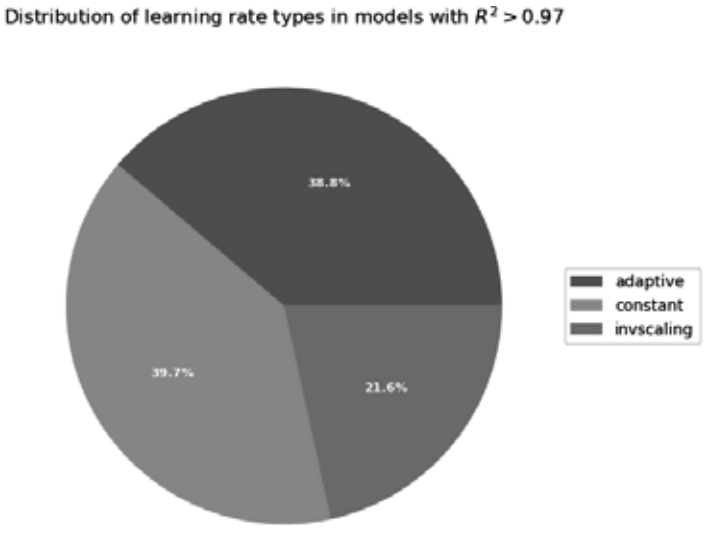

Figure 4 - Distribution of learning rate types variations in the 116 models that satisfy the condition

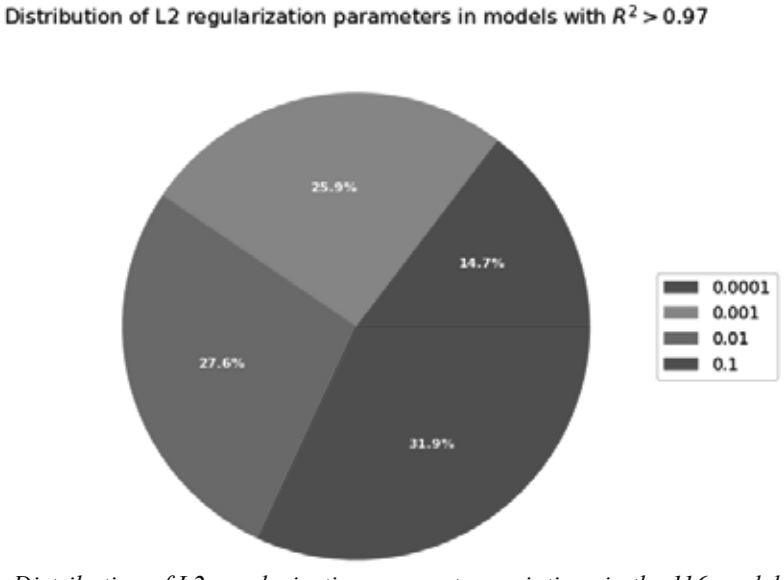

Figure 5 - Distribution of L2 regularization parameter variations in the 116 models that satisfy the condition

The best achieved R^2 value is 0.99329. The Bland-Altman plot for that model is shown in Figure 6. A BA analysis shows that only three points fall outside the confidence interval when using best model, all in a high value range of predicted values. In a lower range of predicted values all points fall within a 0.95 confidence interval.

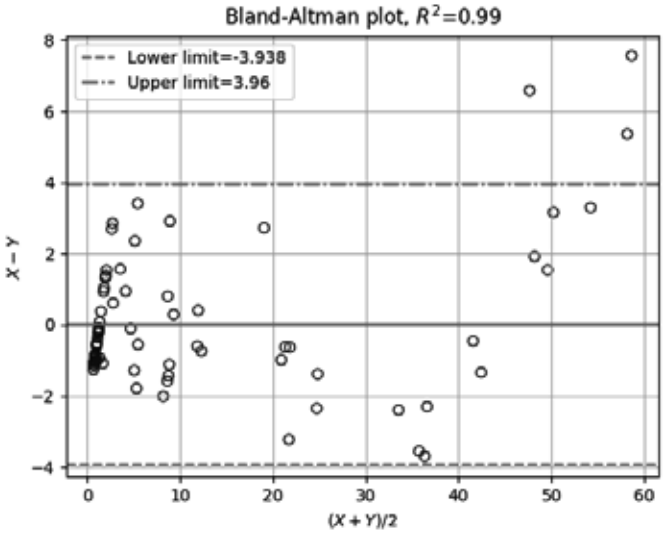

Figure 6 – A Bland-Altman plot for the best model found

Parameters of the best model are given in Table 3.

Table 3 - Parameter values of the best model achieved

Parameter	Value
Hidden layer sizes	(10, 20, 20, 10)
Activation function	relu
Learning rate type	constant
Initial learning rate	0.01
L2	0.001

4. Discussion

Most models tended towards the more complex (10,10,10,10,10) and (10,20,20,10) configurations, with simpler, single hidden layer configurations showing in no models that satisfied the condition. A vast majority of the used models preferred the relu

activation function with the logistic activation function barely being present in the top models. When it comes to learning rate types, the constant and adaptive ones are evenly matched in the observed models, with the inverse scaling having a lower but still significant part in the distribution. Interestingly, the only initial learning rate present in the top 116 models is 0.01, with the other two learning rates not being present at all. Finally, the regularization parameter values are mostly evenly distributed across the models, but there is a slight preference to higher values of L2 parameters.

The best model found shows a very good R^2 value, with the Bland-Altman plot showing only 3 points out of 77 in the training set - (3.89%) are outside of the confidence interval. Those data points are in the higher variable value. The cause of this is the lack of values for the higher range of the output variable value in the data set, as can be seen in Figures 1 and 7.

5. Conclusion

The paper shows a successful application of an MLP regressor on a yacht hydrodynamics data set. It is shown that it is possible to achieve high R^2 values on the given data set with satisfying BA graph results. Best models out of 23040 trained ones have a tendency towards the higher complexity ANNs, with higher regularization parameter value, a 0.01 initial learning rate, with the adaptive or constant typing and relu activation function. The models show the lack of precision in the higher range of the output variable, due to the lower amount of such data in the data set.

Acknowledgements

This research has been (partly) supported by the CEEPUS network CIII-HR-0108, the European Regional Development Fund under the grant KK.01.1.1.01.0009 (DATACROSS) and the University of Rijeka scientific grant uniri-tehnic-18-275-1447.

The data set used in this paper has been obtained from UCI Machine Learning Repository [http://archive.ics.uci.edu/ml]. Dua, D. and Graff, C. (2019), Irvine, CA: University of California, School of Information and Computer Science [3, 4].

References

1. Amedeo Migali, Salvatore Miranda, and Claudio Pensa. Experimental study on the efficiency of trimaran configuration for high-speed very large ships. Proceedings of Fast, RINA, Southampton, pages 4–6, 2001.
2. Jerome H Milgram. Fluid mechanics for sailing vessel design. Annual Review of Fluid Mechanics, 30(1):613–653, 1998.
3. J Gerritsma, R Onnink, and A Versluis. Geometry, resistance and stability of the delft systematic yacht hull series. International shipbuilding progress, 28(328):276–297, 1981.
4. I Ortigosa, R Lopez, and J Garcia. A neural networks approach to residuary resistance of sailing yachts prediction. In Proceedings of the international conference on marine engineering MARINE,

volume 2007, page 250, 2007.
5. Korino Bogović, Ivan Lorencin, Nikola Anđelić, Sebastijan Blažević, Klara Smolčić, Josip Španjol, and Zlatan Car. Artificial intelligence-based method for urinary bladder cancer diagnostic. In International Conference on Innovative Technologies, IN-TECH 2018, 2018.
6. Lorencin, I., Car, Z., Kudláček, J., Mrzljak, V., Anđelić, N., Blažević, S.: Estimation of combined cycle power plant power output using multilayer perceptron variations, 10th International Technical Conference - Technological Forum 2019 - Proceedings, Hlinsko, Czech Republic, p. 94-98, 2019.
7. Lorencin, I., Anđelić, N., Španjol, J., & Car, Z. (2019). Using multi-layer perceptron with Laplacian edge detector for bladder cancer diagnosis. *Artificial Intelligence in Medicine*, 101746.
8. Yufei Wei, Xiaotong Nie, Motoaki Hiraga, Kazuhiro Ohkura, and Zlatan Car. Developing end-to-end control policies for robotic swarms using deep q-learning. Journal of Advanced Computational Intelligence and Intelligent Informatics, 23(5):920–927, 2019.
9. Nikola Anđelić, Sebastijan Blažević, and Zlatan Car. Trajectory planning using genetic algorithm for three joints robot manipulator. In International Conference on Innovative Technologies, IN-TECH 2018, 2018.
10. Lorencin, I., Anđelić, N., Mrzljak, V., & Car, Z. (2019). Genetic Algorithm Approach to Design of Multi-Layer Perceptron for Combined Cycle Power Plant Electrical Power Output Estimation. *Energies*, *12*(22), 4352.
11. Ivan Lorencin, Nikola Anđelić, Vedran Mrzljak, and Zlatan Car. Marine objects recognition using convolutional neural networks. NAŠE MORE: znanstveno-stručni časopis za more i pomorstvo, 66(3):112–119, 2019.
12. Mrzljak, V., Blecich, P., Anđelić, N., & Lorencin, I. (2019). Energy and Exergy Analyses of Forced Draft Fan for Marine Steam Propulsion System during Load Change. *Journal of Marine Science and Engineering*, *7*(11), 381.
13. Bukovac, O., Medica, V., Mrzljak, V.: Steady state performances analysis of modern marine two-stroke low speed diesel engine using MLP neural network model, Shipbuilding: Theory and Practice of Naval Architecture, Marine Engineering and Ocean Engineering 66 (4), p. 57-70, 2015. (https://hrcak.srce.hr/149804)
14. Mrzljak, V., Poljak, I., Prpić-Oršić, J.: Exergy analysis of the main propulsion steam turbine from marine propulsion plant, Shipbuilding: Theory and Practice of Naval Architecture, Marine Engineering and Ocean Engineering 70 (1), p. 59-77, 2019. (doi:10.21278/brod70105)
15. Senčić, T., Mrzljak, V., Blecich, P., Bonefačić, I.: 2D CFD Simulation of Water Injection Strategies in a Large Marine Engine, Journal of Marine Science and Engineering, 7, 296, 2019. (doi:10.3390/jmse7090296)
16. Mrzljak, V., Mrakovčić, T.: Comparison of COGES and Diesel-Electric Ship Propulsion Systems, Journal of Maritime & Transportation Sciences, Special edition No. 1, 2016. (doi:10.18048/2016-00.131)
17. Lorencin, I., Anđelić, N., Mrzljak, V., Car, Z.: Exergy analysis of marine steam turbine labyrinth (gland) seals, Scientific Journal of Maritime Research 33 (1), p. 76–83, 2019. (doi:10.31217/p.33.1.8)
18. Blažević, S., Mrzljak, V., Anđelić, N., Car, Z.: Comparison of energy flow stream and isentropic method for steam turbine energy analysis, Acta Polytechnica 59 (2), p. 109-125, 2019. (doi:10.14311/AP.2019.59.0109)
19. Mrzljak, V., Anđelić, N., Poljak, I., Orović, J.: Thermodynamic analysis of marine steam power plant pressure reduction valves, Journal of Maritime & Transportation Sciences 56 (1), p. 9-30, 2019. (doi:10.18048/2019.56.01)
20. Orović, J., Mrzljak, V., Poljak, I.: Efficiency and Losses Analysis of Steam Air Heater from Marine Steam Propulsion Plant, Energies 2018, 11, 3019. (doi:10.3390/en11113019)
21. Mrzljak, V., Orović, J., Poljak, I., Lorencin, I.: Exergy analysis of steam turbine governing valve from a super critical thermal power plant, XXVII International Scientific Conference Trans & MOTAUTO '19 - PROCEEDINGS, Sofia, Bulgaria p. 99-102, 2019.
22. Poljak, I., Orović, J., Mrzljak, V.: Energy and Exergy Analysis of the Condensate Pump During Internal Leakage from the Marine Steam Propulsion System, Scientific Journal of Maritime Research 32 (2), p. 268-280, 2018. (doi:10.31217/p.32.2.12)
23. Elizabeta Lazarevska. Comparison of different models for residuary resistance prediction. In Proceedings of The 9th EUROSIM Congress on Modelling and Simulation, EUROSIM 2016, The

57th SIMS Conference on Simulation and Modelling SIMS 2016, number 142, pages 511–517. Linköping University Electronic Press, 2018.
24. Even Wollebæk Førrisdal. Empirical prediction of residuary resistance of fast catamarans. Master's thesis, NTNU, 2018.
25. CD Obreja and AM Chirosca. Theoretical and experimental comparative analyse on the hydrodynamic resistance of a racing sailboat. In IOP Conference Series: Materials Science and Engineering, volume 400, page 042044. IOP Publishing, 2018.
26. Jong-hyun Lee, Sung-soo Kim, Soon-sup Lee, Donghoon Kang, and Jaechul Lee. Prediction of added resistance using genetic programming. Ocean Engineering, 153:104–111, 2018.
27. Yinpo Yan and Yuan Chen. Hydrodynamic coefficients calculation of complex-shaped auv based on the Lattice Boltzmann method. In IFToMM International Conference on Mechanisms, Transmissions and Applications, pages 566–575. Springer, 2019.
28. Dheeru Dua and Casey Graff. UCI machine learning repository, 2017.
29. Liang Yun, Alan Bliault, and Huan Zong Rong. Buoyancy and stability. In High Speed Catamarans and Multihulls, pages 71–92. Springer, 2019.
30. Byung Suk Lee. Basic ship geometry. In Hydrostatics and Stability of Marine Vehicles, pages 1–12. Springer, 2019.
31. Guan Guan, Qu Yang, Xiaole Yang, and Yunlong Wang. A new method for parametric design of hull surface based on energy optimization. Journal of Marine Science and Technology, 24(2):424–436, 2019.
32. Pieter Mario Fernandez, Wasis Dwi Aryawan, and Gita Marina Ahadyanti. Desain fast displacement ship untuk lomba kapal cepat pada hydrocontest. Jurnal Teknik ITS, 7(2):G192–G196, 2019.
33. Sotiris Skoupas, George Zaraphonitis, and Apostolos Papanikolaou. Parametric design and optimisation of high-speed ro-ro passenger ships. OceanEngineering, 189:106346, 2019.
34. MJ Legaz, A Querol, and B Flethes. Ship design challenges for ESPOmar project: A review of available methods. Advances in Marine Navigation and Safety of Sea Transportation, page 123, 2019.
35. Hafizul Islam and Guedes Soares. Effect of trim on container ship resistance at different ship speeds and drafts. Ocean Engineering, 183:106–115, 2019.
36. Jiayi He, Huiyu Wu, Chao Ma, Chen-Jun Yang, Renchuan Zhu, Wei Li, and Francis Noblesse. Froude number, hull shape, and convergence of integral representation of ship waves. European Journal of Mechanics-B/Fluids, 78:216–229, 2019.
37. Savas Sezen and Ferdi Cakici. Numerical prediction of total resistance using full similarity technique. China Ocean Engineering, 33(4):493–502, 2019.
38. Lothar Birk. Fundamentals of Ship Hydrodynamics: Fluid Mechanics, Ship Resistance and Propulsion. John Wiley & Sons, 2019.
39. C Celik, DB Danisman, P Kaklis, and S Khan. An investigation into the effect of the hull vane on the ship resistance in openfoam. In Sustainable Development and Innovations in Marine Technologies: Proceedings of the 18th International Congress of the Maritime Association of the Mediterranean (IMAM 2019), September 9-11, 2019, Varna, Bulgaria, page 136. CRC Press, 2019.
40. Francisco Rodrigues Lima-Junior and Luiz Cesar Ribeiro Carpinetti. Predicting supply chain performance based on scor R metrics and multilayer perceptron neural networks. International Journal of Production Economics, 212:19–38, 2019.
41. Ali Asghar Heidari, Hossam Faris, Ibrahim Aljarah, and Seyedali Mirjalili. An efficient hybrid multilayer perceptron neural network with grasshopper optimization. Soft Computing, 23(17):7941–7958, 2019.
42. Takaaki Fujita, Atsushi Sato, Akira Narita, Toshimasa Sone, Kazuaki Iokawa, Kenji Tsuchiya, Kazuhiro Yamane, Yuichi Yamamoto, Yoko Ohira, and Koji Otsuki. Use of a multilayer perceptron to create a prediction model for dressing independence in a small sample at a single facility. Journal of physical therapy science, 31(1):69–74, 2019.
43. Ishteaque Alam, Dewan Md Farid, and Rosaldo JF Rossetti. The prediction of traffic flow with regression analysis. In Emerging Technologies in Data Mining and Information Security, pages 661–671. Springer, 2019.
44. JF Torres, D Gutiérrez-Avilés, A Troncoso, and F Martínez-Álvarez. Random hyper-parameter search-based deep neural network for power consumption forecasting. In International Work-Conference on Artificial Neural Networks, pages 259–269. Springer, 2019.

45. Hoang Nguyen and Xuan-Nam Bui. Predicting blast-induced air overpressure: a robust artificial intelligence system based on artificial neural networks and random forest. Natural Resources Research, 28(3):893–907, 2019.
46. Trevor Hastie, Robert Tibshirani, Jerome Friedman, and James Franklin. The elements of statistical learning: data mining, inference and prediction. The Mathematical Intelligencer, 27(2):83–85, 2005.
47. Ömer Faruk Ertuğrul. A novel type of activation function in artificial neural networks: Trained activation function. Neural Networks, 99:148–157, 2018.
48. U Rajendra Acharya, Shu Lih Oh, Yuki Hagiwara, Jen Hong Tan, and Hojjat Adeli. Deep convolutional neural network for the automated detection and diagnosis of seizure using eeg signals. Computers in biology and medicine, 100:270–278, 2018.
49. Noam Shazeer and Mitchell Stern. Adafactor: Adaptive learning rates with sublinear memory cost. arXiv preprint arXiv:1804.04235, 2018.
50. Risto Miikkulainen, Jason Liang, Elliot Meyerson, Aditya Rawal, Daniel Fink, Olivier Francon, Bala Raju, Hormoz Shahrzad, Arshak Navruzyan, Nigel Duffy, et al. Evolving deep neural networks. In Artificial Intelligence in the Age of Neural Networks and Brain Computing, pages 293–312. Elsevier, 2019.
51. Oleg Sysoev and Oleg Burdakov. A smoothed monotonic regression via l2 regularization. Knowledge and Information Systems, 59(1):197–218, 2019.
52. Hao Li, Zheng Xu, Gavin Taylor, Christoph Studer, and Tom Goldstein. Visualizing the loss landscape of neural nets. In Advances in Neural Information Processing Systems, pages 6389–6399, 2018.
53. Ian Goodfellow, Yoshua Bengio, and Aaron Courville. Deep Learning. MIT Press, 2016.
54. Fabian Pedregosa, Gaël Varoquaux, Alexandre Gramfort, Vincent Michel, Bertrand Thirion, Olivier Grisel, Mathieu Blondel, Peter Prettenhofer, Ron Weiss, Vincent Dubourg, et al. Scikit-learn: Machine learning in python. Journal of machine learning research, 12(Oct):2825–2830, 2011.
55. Mateusz Buda, Atsuto Maki, and Maciej A Mazurowski. A systematic study of the class imbalance problem in convolutional neural networks. Neural Networks, 106:249–259, 2018.
56. Luke Plonsky and Hessameddin Ghanbar. Multiple regression in l2 research: A methodological synthesis and guide to interpreting r2 values. The Modern Language Journal, 102(4):713–731, 2018.
57. Colin B Fogarty. Regression-assisted inference for the average treatment effect in paired experiments. Biometrika, 105(4):994–1000, 2018.
58. Hiroshi Nakano, Tomokazu Furukawa, and Takeshi Tanigawa. Tracheal sound analysis using a deep neural network to detect sleep apnea. Journal of Clinical Sleep Medicine, 15(08):1125–1133, 2019.
59. Amrinder Kaur, Yadwinder Singh Brar, and G Leena. Fault detection in power transformers using random neural networks. International Journal of Electrical and Computer Engineering, 9(1):78, 2019.
60. Jay Hertel. A picture tells 1000 words (but most results graphs do not): 21 alternatives to simple bar and line graphs. Clinics in sports medicine, 37(3):441–462, 2018.